Impact of Hydrophobic and Electrostatic Forces on the Adsorption of *Acacia* Gum on Oxide Surfaces Revealed by QCM-D

Athénaïs Davantès [1,*], Michaël Nigen [2], Christian Sanchez [2] and Denis Renard [1]

[1] INRAE, UR BIA, F-44316 Nantes, France; denis.renard@inrae.fr (D.R.)
[2] UMR IATE, Université Montpellier, INRAE, Institut Agro, 34060 Montpellier, France
* Correspondence: athenais.davantes@inrae.fr

Table S1. Biochemical composition and structural parameters of A. *senegal* and A. *seyal* gums.

	A. *senegal* [1]	**A. *seyal*** [2]
Moisture (%)	10.7	11.4
Sugar (%)		
Arabinose	29.8	47.6
Galactose	38.5	36.9
Rhamnose	12.8	3.0
Glucuronic acid	17.9	6.7
4-O-Me-Glucuronic acid	1.0	5.8
Uronic acid / neutral sugar ratio	0.23	0.14
Protein (%)[a]	2.0	1.0
Mineral (%)	3.3	4.0
Weight-average molecular weight (M_w, g.mol^{-1})	6.5×10^5	8.2×10^5
Polydispersity index (M_w/M_n)	2.2	1.5
High M_w AGP (%)	15.4	20
Branching degree (%)	78.0	59.2
Intrinsic viscosity (mL.g^{-1}) [b]	30.2	16.5
Number of negative charges	560	452
R_g (nm)	28.6	17.1
R_h (nm)		
Dynamic light scattering	15[c], 16[d]	13[c], 14[d]
Viscosimetry	15	14
Partial specific volume $v_s°$ (cm^3.g^{-1})	0.5870	0.5767
Density	1.703	1.734
Partial specific adiabatic compressibility coefficient $\beta_s°$ (x10^{11}.Pa^{-1})	-12.2	-13.2

[1] from Apolinar-Valiente et al. (2019) Food Hydrocolloids 89 pp. 864-873

[2] from Lopez Torrez et al. (2015) Food Hydrocolloids 51 pp. 41-53

[a] Protein content was measured using the Kjeldhal method

[b] Measured using differential capillary viscometry (on line size exclusion chromatography system) in 100 mM $LiNO_3$ (pH 5.0) solution containing 0.02% NaN_3

[c] Hydrodynamic radius (R_h) in sodium acetate 10 mM pH 5

[d] Hydrodynamic radius (R_h) in 100 mM $LiNO_3$ (pH 5.0)

Figure S1. AFM topology images of quartz sensor surfaces

Surfaces	AFM topology images 3D
Au	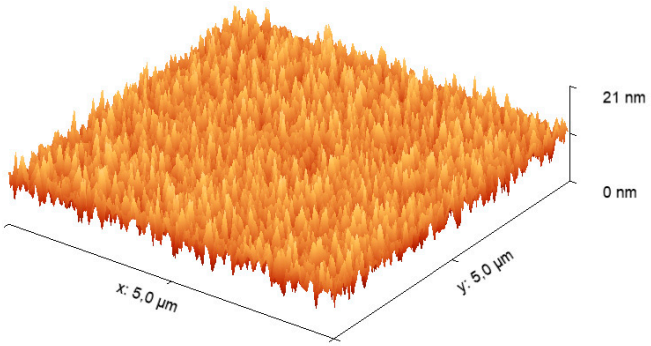
SiO_2	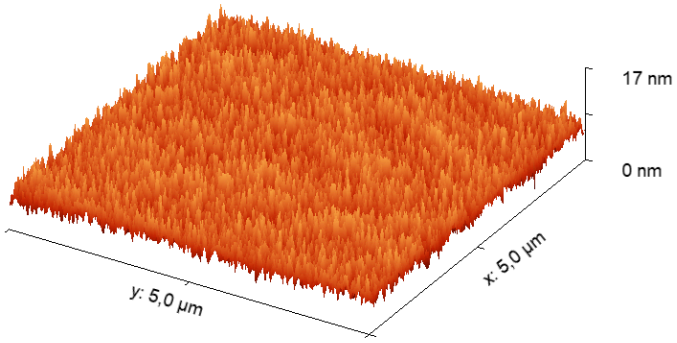
TiO_2	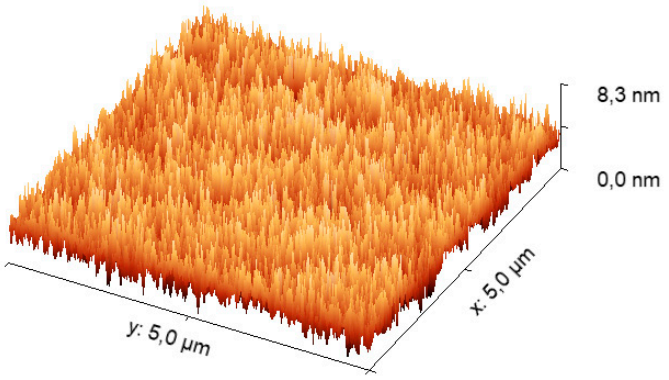

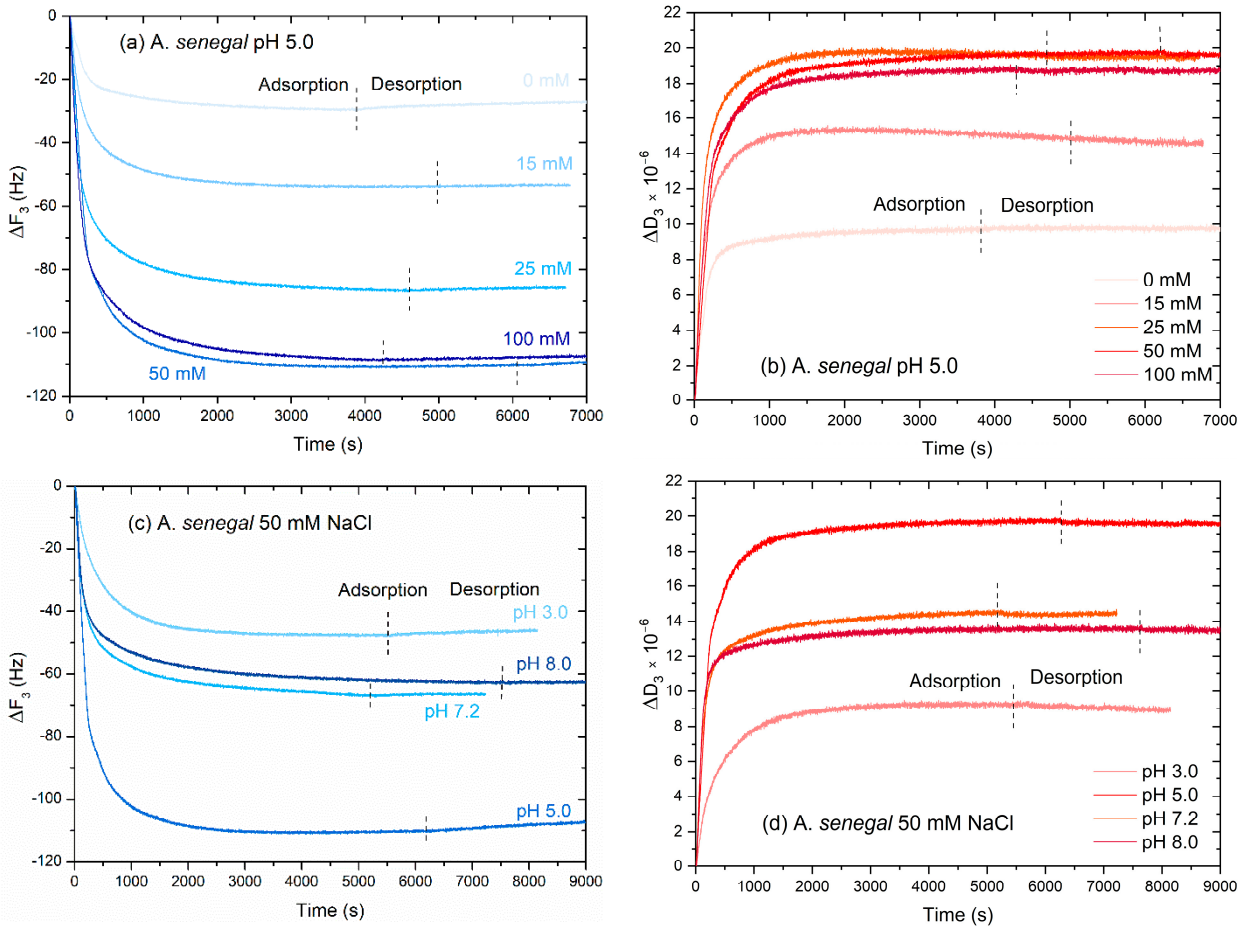

Figure S2. Adsorption of A. *senegal* gum at 150 ppm on **gold** substrate at pH 5.0: (a) frequency change (ΔF) and (b) dissipation energy loss (ΔD) for the third overtone at 0, 15, 25, 50 and 100 mM NaCl and at 50 mM NaCl for pH 3.0, 5.0, 7.2 and 8.0 with (c) ΔF and (d) ΔD. Dashed lines represent the switch of solution from adsorption to desorption process with initial buffer.

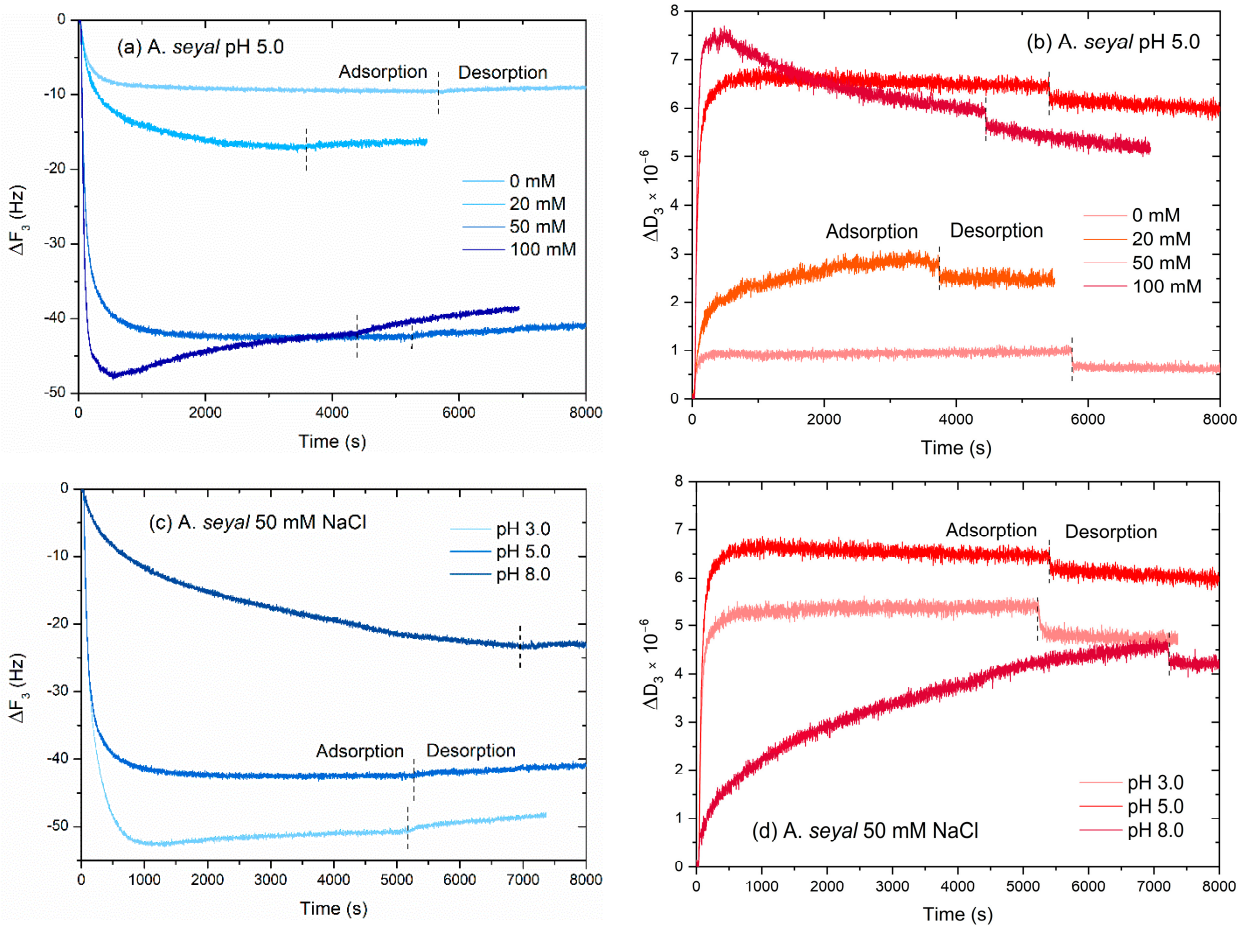

Figure S3. Adsorption of A. *seyal* gum at 500 ppm on **gold** substrate at pH 5.0: (a) frequency change (ΔF) and (b) dissipation energy loss (ΔD) for the third overtone at 0, 20, 50 and 100 mM NaCl and at 50 mM NaCl for pH 3.0, 5.0 and 8.0 with (c) ΔF and (d) ΔD. Dashed lines represent the switch of solution from adsorption to desorption process with initial buffer.

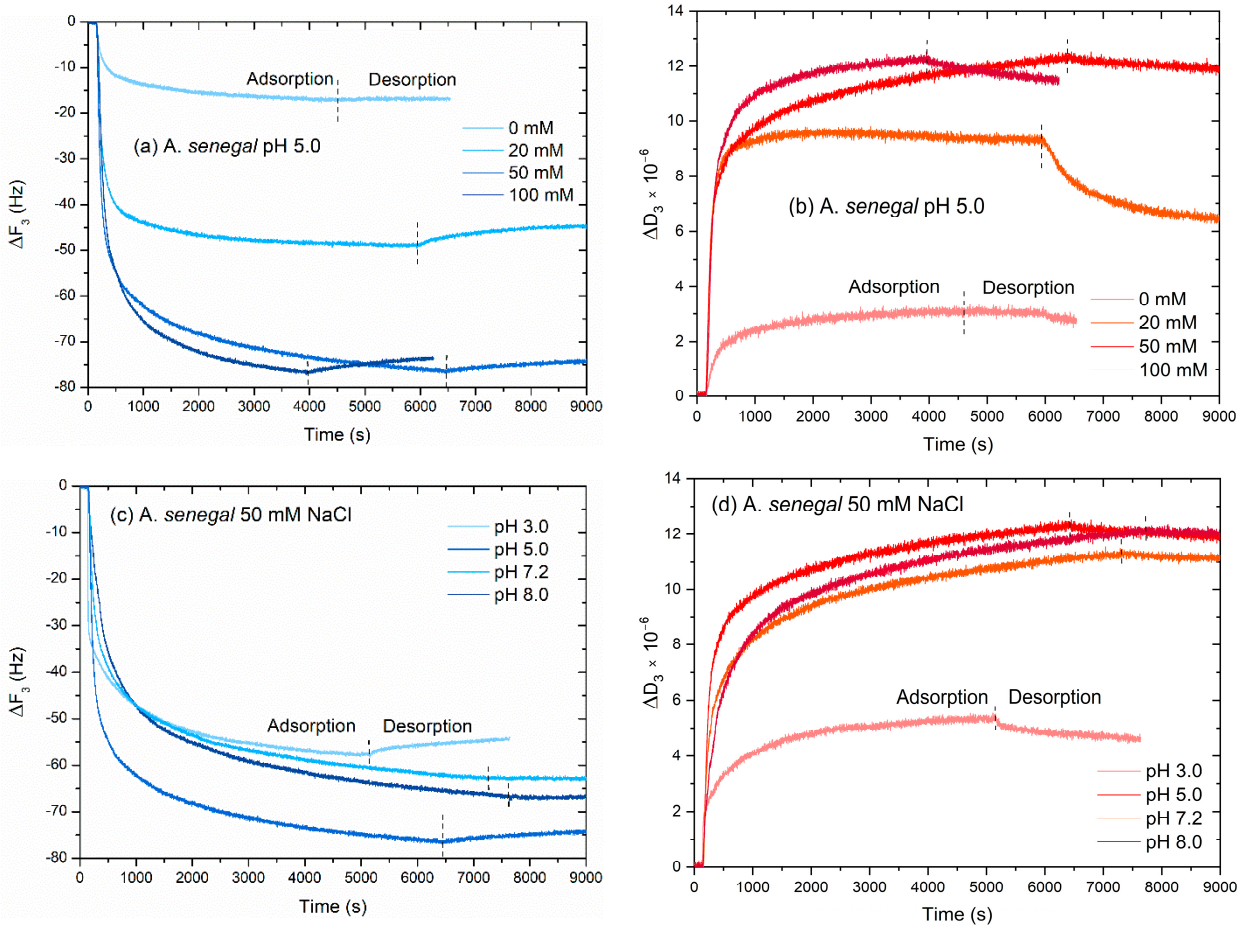

Figure S4. Adsorption of A. *senegal* gum at 150 ppm on TiO_2 substrate at pH 5.0: (a) frequency change (ΔF) and (b) dissipation energy loss (ΔD) for the third overtone at 0, 20, 50 and 100 mM NaCl and at 50 mM NaCl for pH 3.0, 5.0, 7.2 and 8.0 with (c) ΔF and (d) ΔD. Dashed lines represent the switch of solution from adsorption to desorption process with initial buffer.

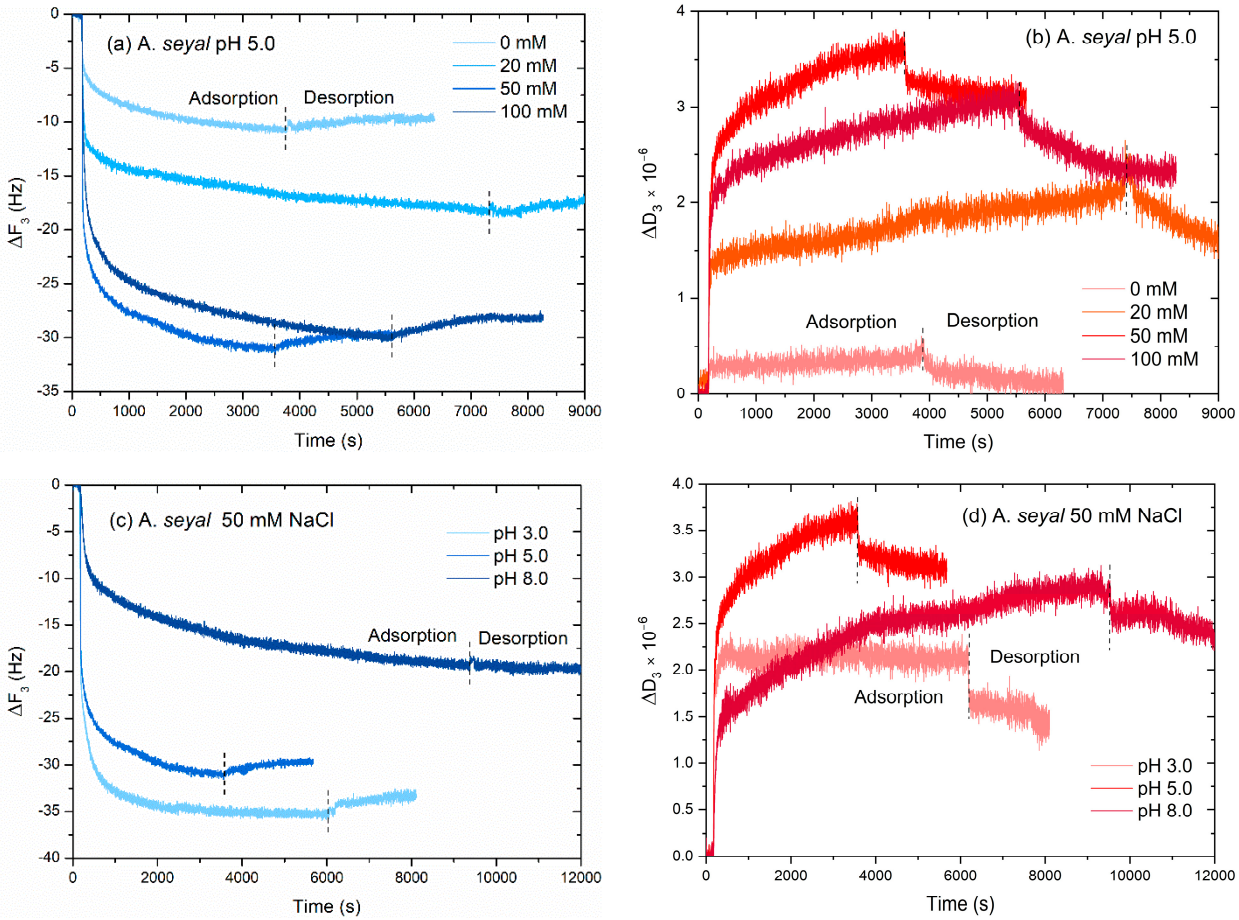

Figure S5. Adsorption of A. *seyal* gum at 500 ppm on TiO_2 substrate at pH 5.0: (a) frequency change (ΔF) and (b) dissipation energy loss (ΔD) for the third overtone at 0, 20, 50 and 100 mM NaCl and at 50 mM NaCl for pH 3.0, 5.0 and 8.0 with (c) ΔF and (d) ΔD. Dashed lines represent the switch of solution from adsorption to desorption process with initial buffer.

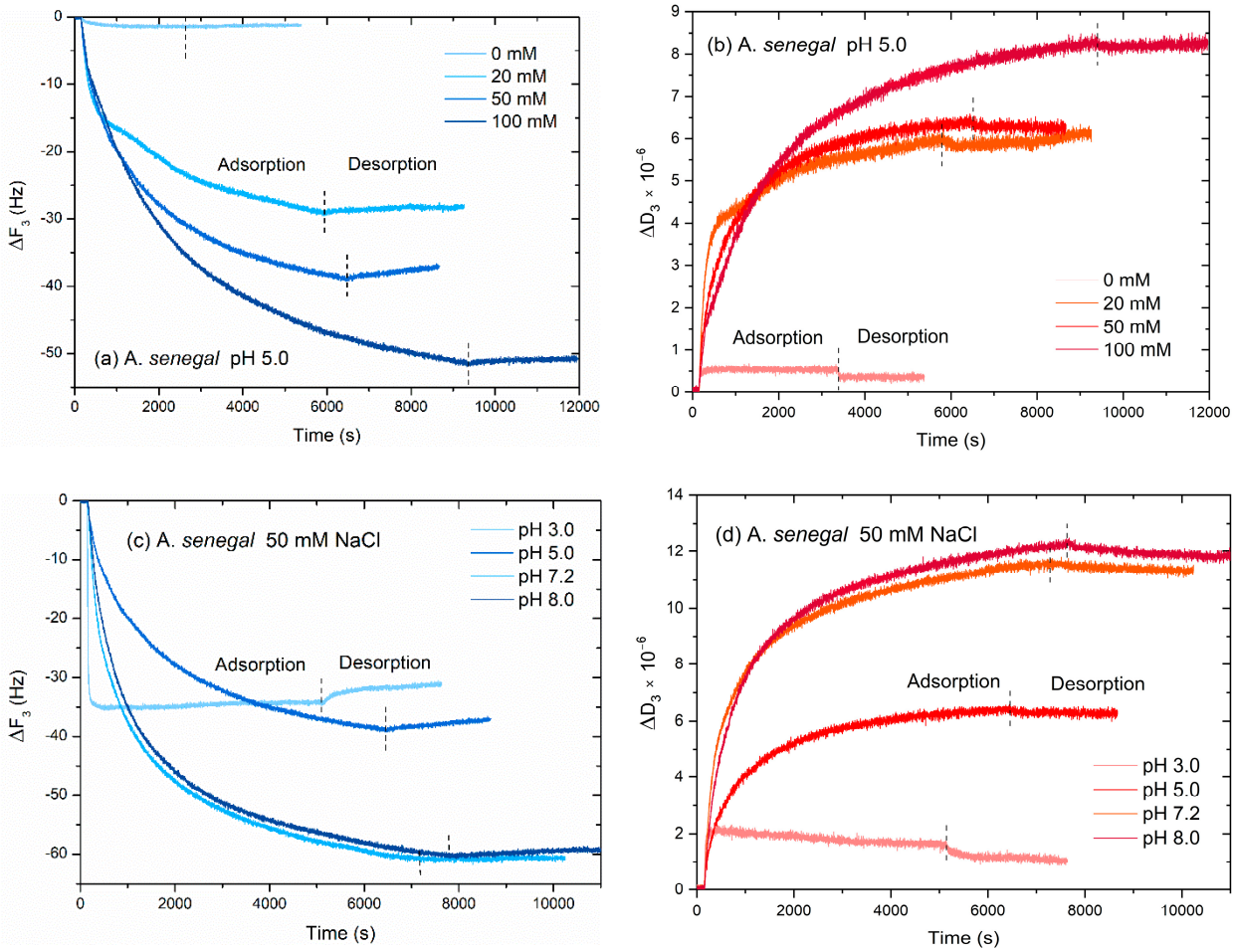

Figure S6. Adsorption of A. *senegal* gum at 150 ppm on **SiO_2** substrate at pH 5.0: (a) frequency change (ΔF) and (b) dissipation energy loss (ΔD) for the third overtone at 0, 20, 50 and 100 mM NaCl and at 50 mM NaCl for pH 3.0, 5.0, 7.2 and 8.0 with (c) ΔF and (d) ΔD. Dashed lines represent the switch of solution from adsorption to desorption process with initial buffer.

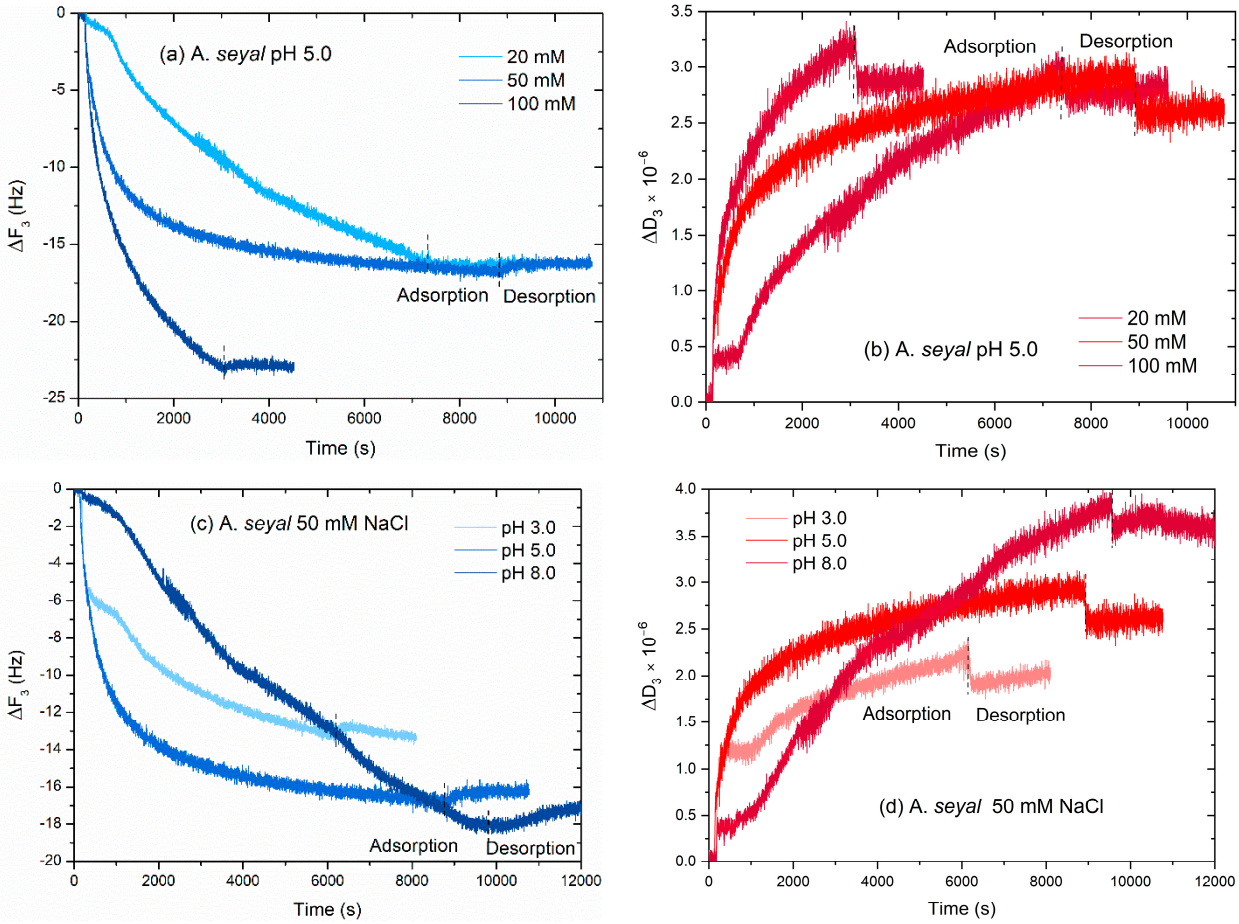

Figure S7. Adsorption of A. *seyal* gum at 500 ppm on **SiO_2** substrate at pH 5.0: (a) frequency change (ΔF) and (b) dissipation energy loss (ΔD) for the third overtone at 20, 50 and 100 mM NaCl and at 50 mM NaCl for pH 3.0, 5.0 and 8.0 with (c) ΔF and (d) ΔD. Dashed lines represent the switch of solution from adsorption to desorption process with initial buffer.

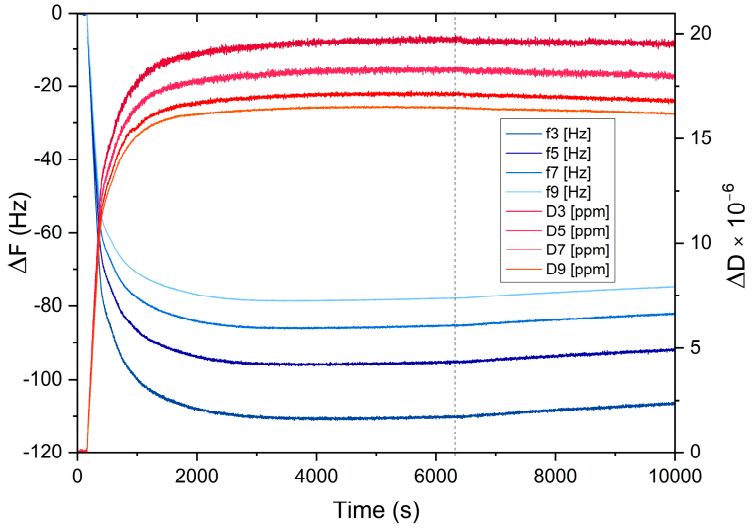

Figure S8. Adsorption of A. *senegal* gum at 150 ppm 10 mM acetate buffer and 50 mM NaCl pH 5.0 on **gold** substrate: frequency change (ΔF) and dissipation energy loss (ΔD) in time for four overtone frequencies.

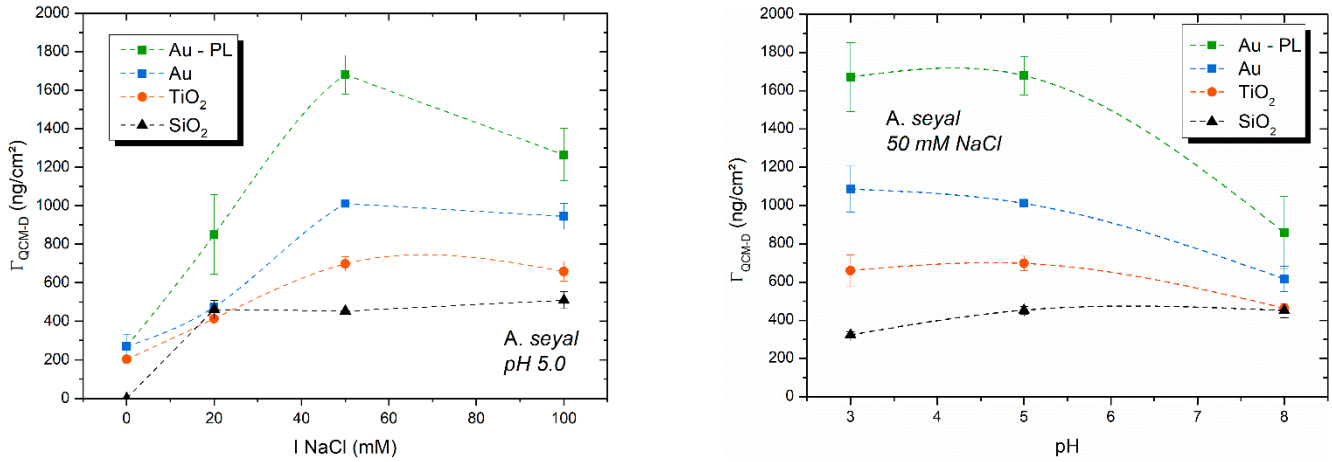

Figure S9. Adsorbed amount (Γ_{QCM-D}) onto Au substrate with the power-law model (-■-), compare to Voigt Model on Au (-■-), TiO_2 (-●-) and SiO_2 (-▲-) at equilibrium state in function of NaCl ionic strength (left), and pH (right) for A. *seyal* gum. *Lines are guides for the eyes.*

Table S2. QCM-D data of A. *senegal* films after adsorption on **gold** at pH 5.0 in function of ionic strength in NaCl.

A. *senegal*					
pH 5.0	**0 mM NaCl**	**15 mM NaCl**	**25 mM NaCl**	**50 mM NaCl**	**100 mM NaCl**
10 mM acetate					
Model	**Power-law**	**Power-law**	**Power-law**	**Power-law**	**Power-law**
Γ_{QCM-D} (ng/cm²)	1533.7 ± 152.2	2596.0 ± 153.6	3144.0 ± 64.6	3215.9 ± 313.8	3270.2 ± 272.4
d_{QCM-D} (nm)	9.00 ± 0.89	15.24 ± 0.90	18.46 ± 0.38	18.9 ± 1.8	19.2 ± 1.6
Desorption QCM-D	1.5 %	1.7 %	0.7 %	1.2 %	2.5 %
Shear viscosity η (μPa.s)	845.0 ± 13.2	986.7 ± 15.3	1160.7 ± 19.4	1348.8 ± 106.9	1363.0 ± 34.2
Shear elastic modulus μ (kPa)	23.2 ± 3.8	21.3 ± 1.15	34.2 ± 5.1	41.8 ± 12.3	43.8 ± 9.7
χ^2	0.34 ± 0.23	0.73 ± 0.55	1.33 ± 1.56	0.85 ± 0.67	0.90 ± 1.29
Number of Regimes	3	4	4	3	3

(D-f plot)				

Table S3. QCM-D data of A. *senegal* films after adsorption on **gold** with 50 mM NaCl in function of pH.

A. *senegal*				
10 mM acetate	**pH 3.0**	**pH 5.0**	**pH 7.2**	**pH 8.0**
50 mM NaCl				
Model	**Power-law**	**Power-law**	**Power-law**	**Power-law**
Γ_{QCM-D} (ng/cm²)	1739.2 ± 120.6	3215.9 ± 313.8	2413.8 ± 138.36	1957.0 ± 154.8
d_{QCM-D} (nm)	10.21 ± 0.71	18.9 ± 1.8	14.17 ± 0.81	11.49 ± 0.91
Desorption QCM-D	1.1 %	1.2 %	0 %	2.3 %
Shear viscosity η (μPa.s)	1203.6 ± 44.1	1348.8 ± 106.9	1150.0 ± 16.6	1137.4 ± 32.09
Shear elastic modulus μ (kPa)	30.9 ± 6.7	41.8 ± 12.3	34.4 ± 5.1	36.1 ± 9.7
χ^2	0.11 ± 0.05	0.85 ± 0.67	0.28 ± 0.13	0.63 ± 0.50
Number of Re-gimes (D-f plot)	3	3	2	3

Table S4. QCM-D data of A. *seyal* films after adsorption on **gold** at pH 5.0 in function of ionic strength in NaCl.

A. *seyal*							
pH 5.0	**0 mM NaCl**	**20 mM NaCl**		**50 mM NaCl**		**100 mM NaCl**	
10 mM ace-tate							
Model	**Voigt**	**Voigt**	**Power-law**	**Voigt**	**Power-law**	**Voigt**	**Power-law**

Γ_{QCM-D} (ng/cm²)	269.3 ± 62.8	474.1 ± 17.8	850.2 ± 206.5	1011.3 ± 14.9	1679.6 ± 101.1	944.3 ± 66.7	1264.5 ± 136.1
d_{QCM-D} (nm)	1.55 ± 0.36	2.73 ± 0.10	4.90 ± 1.19	5.83 ± 0.09	9.69 ± 0.58	5.45 ± 0.38	7.29 ± 0.79
Desorption QCM-D	15.5 %	10.3 %	18.1 %	8.4 %	15.3 %	10.2 %	17.0 %
Shear viscosity η (μPa.s)	1382.7 ± 305.2	1092.0 ± 6.3	995.0 ± 130.3	1152.7 ± 9.9	1169.3 ± 26.9	1233.0 ± 31.3	1357.0 ± 67.8
Shear elastic modulus μ (kPa)	116.2 ± 68.2	115.5 ± 4.0	16.3 ± 11.2	139.0 ± 4.6	17.8 ± 2.0	149.6 ± 3.6	33.6 ± 9.9
χ^2	0.56 ± 0.72	2.04 ± 0.25	0.16 ± 0.13	9.33 ± 1.15	0.09 ± 0.05	7.02 ± 4.15	0.16 ± 0.04
Number of Regimes (D-f plot)	2	3		4		4	

Table S5. QCM-D data of A. *seyal* films after adsorption on **gold** with 50 mM NaCl in function of pH.

A. *seyal*						
10 mM acetate	**pH 3.0**		**pH 5.0**		**pH 8.0**	
50 mM NaCl						
Model	**Voigt**	**Power-law**	**Voigt**	**Power-law**	**Voigt**	**Power-law**
Γ_{QCM-D} (ng/cm²)	1086.1 ± 120.4	1672.4 ± 180.3	1011.3 ± 14.9	1679.6 ± 101.1	616.2 ± 67.1	858.8 ± 187.6
d_{QCM-D} (nm)	6.26 ± 0.69	9.64 ± 1.04	5.83 ± 0.09	9.69 ± 0.58	3.55 ± 0.39	4.95 ± 1.08
Desorption QCM-D	7.7 %	13.2 %	8.4 %	15.3 %	3.7 %	9.2 %

Shear viscosity η (μPa.s)	1506.5 ± 111.5	1326.3 ± 105.6	1152.7 ± 9.9	1169.3 ± 26.9	964.5 ± 53.7	1034.7 ± 76.9
Shear elastic modulus μ (kPa)	182.6 ± 6.5	19.5 ± 4.1	139.0 ± 4.6	17.8 ± 2.0	112.5 ± 5.1	30.5 ± 15.5
χ^2	6.25 ± 0.64	0.10 ± 0.06	9.33 ± 1.15	0.09 ± 0.05	4.23 ± 0.87	0.27 ± 0.28
Number of Regimes (D-f plot)	4		4		2	

Table S6. QCM-D data of A. *senegal* films after adsorption on TiO_2 at pH 5.0 in function of ionic strength in NaCl.

A. *senegal* pH 5.0 10 mM acetate	**0 mM NaCl**	**20 mM NaCl**	**50 mM NaCl**	**100 mM NaCl**
Model	**Power-law**	**Power-law**	**Power-law**	**Power-law**
Γ_{QCM-D} (ng/cm²)	639.0 ± 55.2	2004.4 ± 55.0	2468.9 ± 171.7	2313.4 ± 166.2
d_{QCM-D} (nm)	3.75 ± 0.32	11.78 ± 0.33	14.49 ± 1.01	13.58 ± 0.98
Desorption QCM-D	11.9 %	15.3 %	4.5 %	6.5 %
Shear viscosity η (μPa.s)	1060.0 ± 17.3	1095.0 ± 7.0	1277.5 ± 94.6	1388.6 ± 40.2
Shear elastic modulus μ (kPa)	23.7 ± 2.3	21.5 ± 3.5	29.5 ± 5.1	39.2 ± 6.6
χ^2	0.10 ± 0.05	0.10 ± 0.00	0.23 ± 0.10	0.27 ± 0.12
Number of Regimes (D-f plot)	2	3	3	3

Table S7. QCM-D data of A. *senegal* films after adsorption on TiO_2 with 50 mM NaCl in function of pH.

A. *senegal*				
10 mM acetate	**pH 3.0**	**pH 5.0**	**pH 7.2**	**pH 8.0**
50 mM NaCl				
Model	**Power-law**	**Power-law**	**Power-law**	**Power-law**
Γ_{QCM-D} (ng/cm²)	1850.2 ± 152.3	2468.9 ± 171.7	2109.9 ± 50.2	2140.3 ± 282.4
d_{QCM-D} (nm)	10.90 ± 0.85	14.49 ± 1.01	12.39 ± 0.30	12.57 ± 1.66
Desorption QCM-D	20.3 %	4.5 %	7.8 %	1.8 %
Shear viscosity η (μPa.s)	1575.0 ± 21.2	1277.5 ± 94.6	1170.0 ± 99.0	1237.0 ± 7.1
Shear elastic modulus μ (kPa)	21.5 ± 5.0	29.5 ± 5.1	29.0 ± 10.0	33.0 ± 4.2
χ^2	0.11 ± 0.04	0.23 ± 0.10	0.18 ± 0.04	0.16 ± 0.03
Number of Re-gimes (D-f plot)	4	3	3	3

Table S8. QCM-D data of A. *seyal* films after adsorption on TiO_2 at pH 5.0 in function of ionic strength in NaCl.

A. *seyal*				
pH 5.0	**0 mM NaCl**	**20 mM NaCl**	**50 mM NaCl**	**100 mM NaCl**
10 mM acetate				
Model	**Voigt**	**Voigt**	**Voigt**	**Voigt**
Γ_{QCM-D} (ng/cm²)	202.7 ± 5.5	413.6 ± 8.1	697.7 ± 37.3	658.7 ± 51.2
d_{QCM-D} (nm)	1.17 ± 0.03	2.39 ± 0.05	4.02 ± 0.22	3.80 ± 0.30
Desorption	16.3 %	15.8 %	9.3 %	12.1 %

QCM-D				
Shear viscosity η (μPa.s)	2240.0 ± 341.8	1332.5 ± 109.6	1385.7 ± 100.9	1531.7 ± 75.9
Shear elastic modulus μ (kPa)	433.3 ± 189.3	185.0 ± 7.1	179.3 ± 38.3	202.3 ± 9.3
χ^2	1.17 ± 0.74	1.25 ± 0.07	2.78 ± 0.90	2.23 ± 0.68
Number of Re-gimes (D-f plot)	2	3	3	3

Table S9. QCM-D data of A. *seyal* films after adsorption on TiO_2 with 50 mM NaCl in function of pH.

A. *seyal*			
10 mM acetate 50 mM NaCl	**pH 3.0**	**pH 5.0**	**pH 8.0**
Model	**Voigt**	**Voigt**	**Voigt**
Γ_{QCM-D} (ng/cm²)	660.5 ± 80.9	697.7 ± 37.3	463.8 ± 4.1
d_{QCM-D} (nm)	3.81 ± 0.47	4.02 ± 0.22	2.67 ± 0.02
Desorption QCM-D	11.5 %	9.3 %	5.2 %
Shear viscosity η (μPa.s)	2432.5 ± 10.6	1385.7 ± 100.9	1095.5 ± 81.3
Shear elastic modulus μ (kPa)	350.0 ± 21.2	179.3 ± 38.3	137.3 ± 6.7
χ^2	1.20 ± 0.00	2.78 ± 0.90	1.93 ± 0.39
Number of Re-gimes	3	3	3

(D-f plot)				

Table S10. QCM-D data of A. *senegal* films after adsorption on **SiO_2** at pH 5.0 in function of ionic strength in NaCl.

A. *senegal*				
pH 5.0	**0 mM NaCl[1]**	**20 mM NaCl**	**50 mM NaCl**	**100 mM NaCl**
10 mM acetate				
Model	**Sauerbrey[1]**	**Power-law**	**Power-law**	**Power-law**
Γ_{QCM-D} (ng/cm²)	21.3 ± 3.1[1]	1298.8 ± 66.8	1737.9 ± 325.1	1670.7 ± 316.4
d_{QCM-D} (nm)	0.13 ± 0.02[1]	7.63 ± 0.39	10.21 ± 1.91	9.81 ± 1.86
Desorption QCM-D	16 %[1]	3.3 %	1.7 %	2.1 %
Shear viscosity η (μPa.s)	-	982.0 ± 2.8	1127.5 ± 135.5	1256.2 ± 83.7
Shear elastic modulus μ (kPa)	-	15.2 ± 1.1	21.7 ± 10.9	29.2 ± 9.4
χ^2	-	0.05 ± 0.01	0.33 ± 0.25	0.17 ± 0.11
Number of Re-gimes (D-f plot)	2	3	3	2

[1]*At 0 mM NaCl the adsorption was too weak to use both the power-law or Voigt model, Sauerbrey equation was therefore used.*

Table S11. QCM-D data of A. *senegal* films after adsorption on **SiO_2** with 50 mM NaCl in function of pH.

A. *senegal*				
10 mM acetate	**pH 3.0**	**pH 5.0**	**pH 7.2**	**pH 8.0**
50 mM NaCl				
Model	**Power-law**	**Power-law**	**Power-law**	**Power-law**

Γ_{QCM-D} (ng/cm²)	706.2 ± 2.9	1737.9 ± 325.1	2229.1 ± 282.0	2176.9 ± 100.0
d_{QCM-D} (nm)	4.15 ± 0.02	10.21 ± 1.91	13.10 ± 1.66	12.78 ± 0.59
Desorption QCM-D	17.4 %	1.7 %	2.0 %	2.5 %
Shear viscosity η (μPa.s)	3362.5 ± 371.2	1127.5 ± 135.5	1167.5 ± 24.7	1144.0 ± 22.6
Shear elastic modulus μ (kPa)	115.0 ± 21.2	21.7 ± 10.9	29.0 ± 7.1	30.2 ± 0.4
χ^2	0.19 ± 0.01	0.33 ± 0.25	0.18 ± 0.04	0.55 ± 0.35
Number of Re-gimes (D-f plot)	3	3	2	2

Table S12. QCM-D data of A. *seyal* films after adsorption on **SiO_2** at pH 5.0 in function of ionic strength in NaCl.

A. *seyal* pH 5.0 10 mM acetate	**0 mM NaCl**	**20 mM NaCl**	**50 mM NaCl**	**100 mM NaCl**
Model	**-**	**Voigt**	**Voigt**	**Voigt**
Γ_{QCM-D} (ng/cm²)	-	460.7 ± 46.6	453.0 ± 20.4	509.3 ± 44.0
d_{QCM-D} (nm)	-	2.66 ± 0.27	2.61 ± 0.12	2.94 ± 0.25
Desorption QCM-D	-	1.6 %	8.6 %	4.1 %
Shear viscosity η (μPa.s)	-	1046.5 ± 40.3	998.3 ± 50.7	1197.5 ± 24.7

Shear elastic modulus μ (kPa)	-	120.5 ± 3.5	129.0 ± 8.8	187.5 ± 24.7
χ^2	-	2.20 ± 0.28	2.43 ± 0.49	1.78 ± 1.17
Number of Re-gimes (D-f plot)	-	3	3	3

Table S13. QCM-D data of A. *seyal* films after adsorption on **SiO_2** with 50 mM NaCl in function of pH.

A. *seyal* 10 mM acetate 50 mM NaCl	**pH 3.0**	**pH 5.0**	**pH 8.0**
Model	**Voigt**	**Voigt**	**Voigt**
Γ_{QCM-D} (ng/cm²)	323.4 ± 15.9	453.0 ± 20.4	450.8 ± 37.5
d_{QCM-D} (nm)	1.87 ± 0.09	2.61 ± 0.12	2.60 ± 0.22
Desorption QCM-D	6.0 %	8.6 %	8.1 %
Shear viscosity η (μPa.s)	1043.5 ± 17.7	998.3 ± 50.7	863.0 ± 35.4
Shear elastic modulus μ (kPa)	126.0 ± 5.7	129.0 ± 8.8	108.0 ± 8.5
χ^2	1.12 ± 0.19	2.43 ± 0.49	3.00 ± 0.00
Number of Re-gimes (D-f plot)	3	3	2

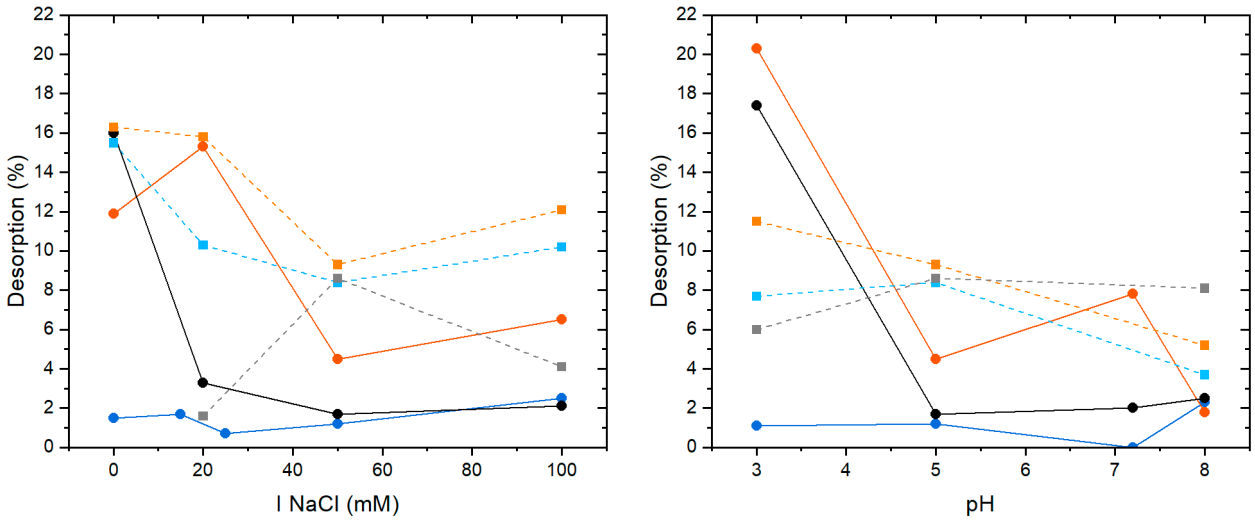

Figure S10. Films desorption (%) as a function of ionic strength at pH 5.0 (left) or as a function of pH with 50 mM NaCl (right) for A. *senegal* with the power-law model (-●-) and A. *seyal* with the Voigt model (--■--) onto gold (blue), TiO_2 (orange) or SiO_2 (black) sensors surface.

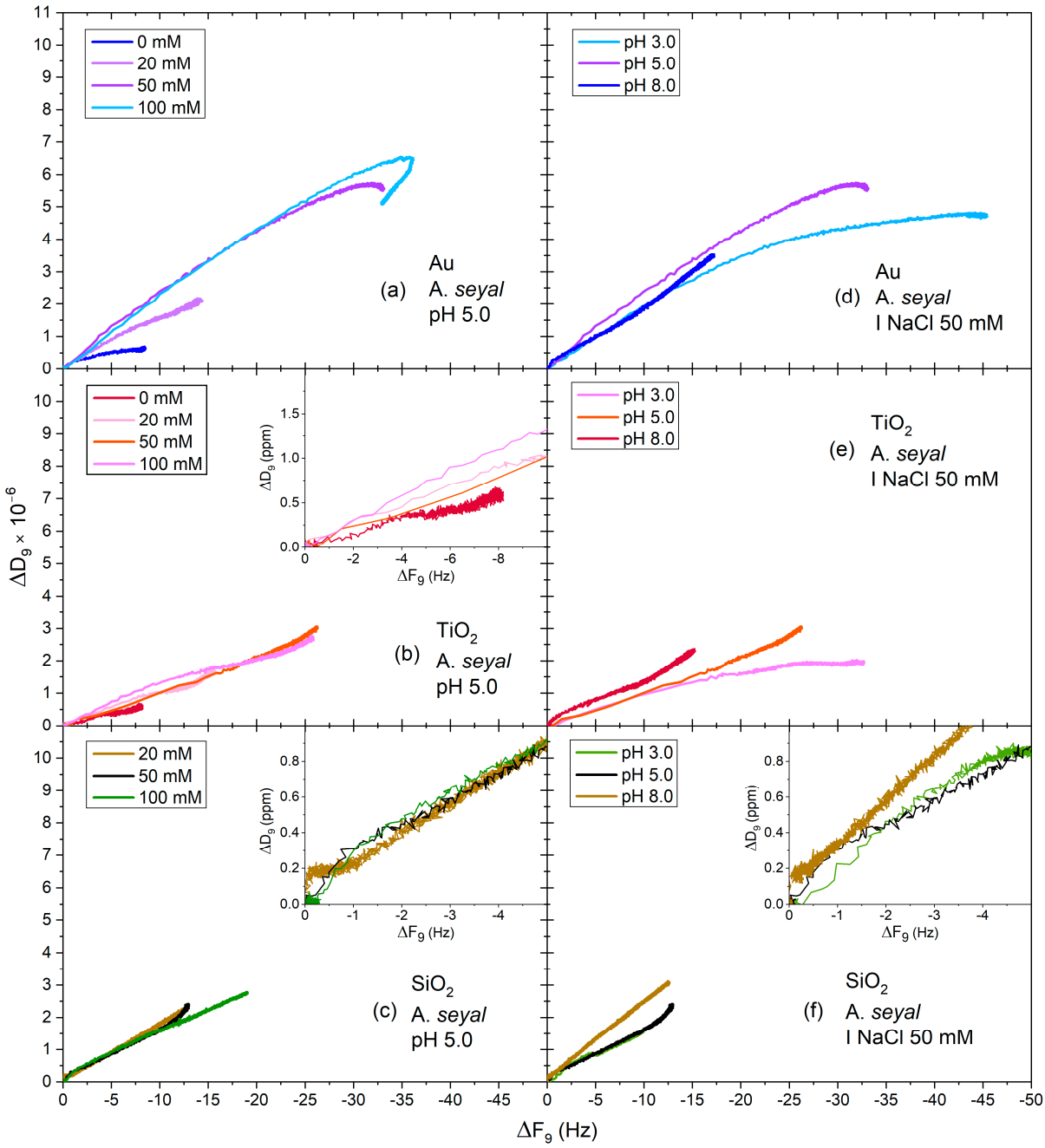

Figure S11. *D-f* plots from the ninth overtone of A. *seyal* in function of ionic strength at pH 5.0 (a, b and c) or in function of pH at 50 mM NaCl (d, e and f) for gold, TiO_2 or SiO_2 sensors surface during the adsorption process.

Figure S12. $|\Delta D/\Delta F|$ *D-f* slopes obtained from a linear fit of the three principal regimes displayed by the $\Delta D/\Delta F$ curves calculated from the ninth overtones for each experimental conditions on the three type of quartz sensors. *Lines are guides for the eyes.*

I NaCl (mM)	pH
Gold	
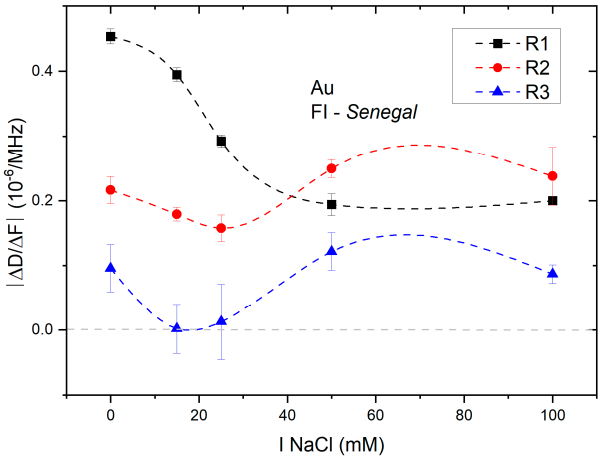	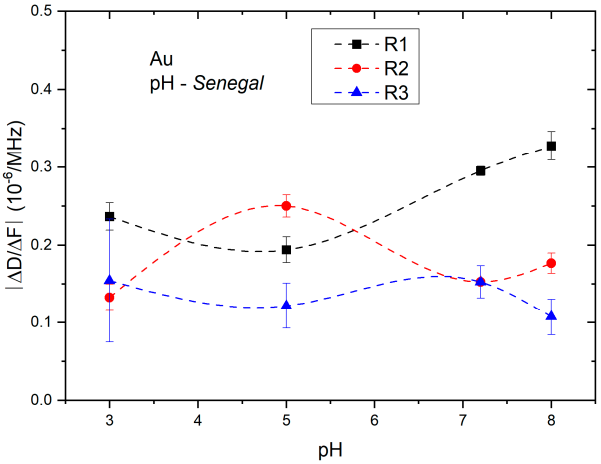
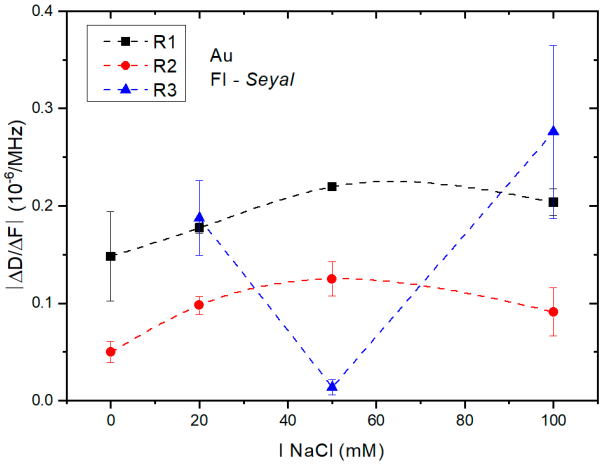	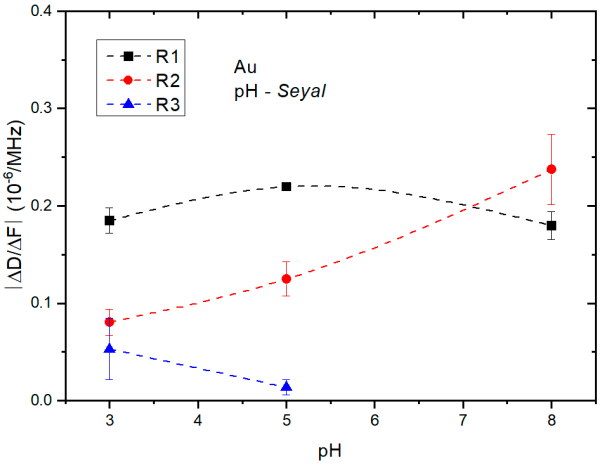

TiO_2

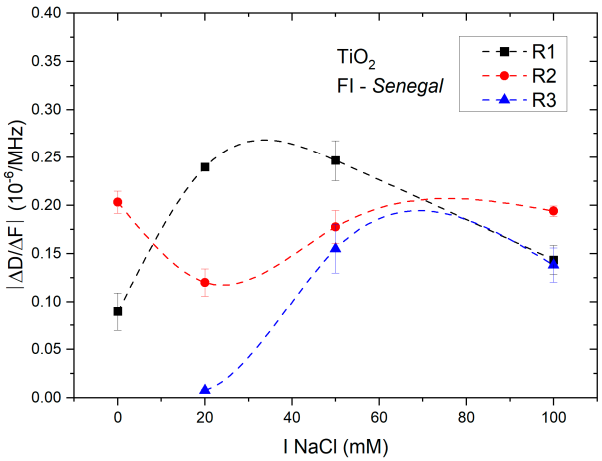
TiO2
FI - Senegal
R1
R2
R3
|ΔD/ΔF| (10-6/MHz)
I NaCl (mM)

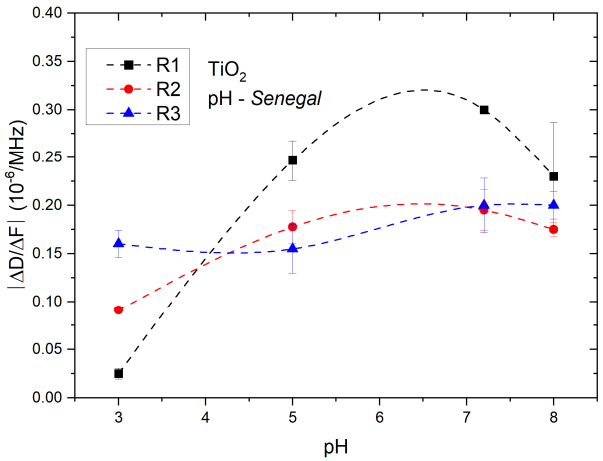
TiO2
pH - Senegal
R1
R2
R3
|ΔD/ΔF| (10-6/MHz)
pH

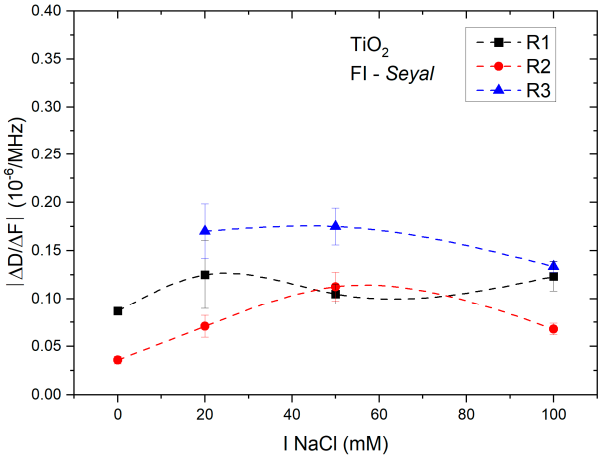
TiO2
FI - Seyal
R1
R2
R3
|ΔD/ΔF| (10-6/MHz)
I NaCl (mM)

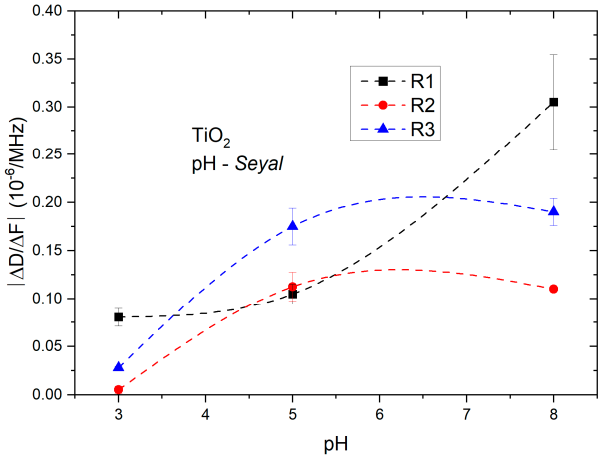
TiO2
pH - Seyal
R1
R2
R3
|ΔD/ΔF| (10-6/MHz)
pH

SiO_2

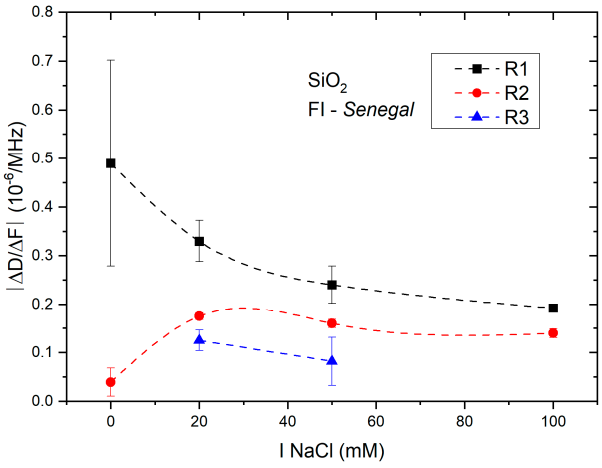
SiO2
FI - Senegal
R1
R2
R3
|ΔD/ΔF| (10-6/MHz)
I NaCl (mM)

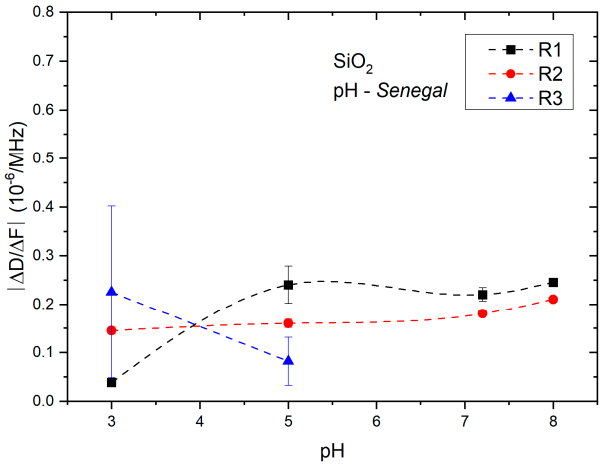
SiO2
pH - Senegal
R1
R2
R3
|ΔD/ΔF| (10-6/MHz)
pH

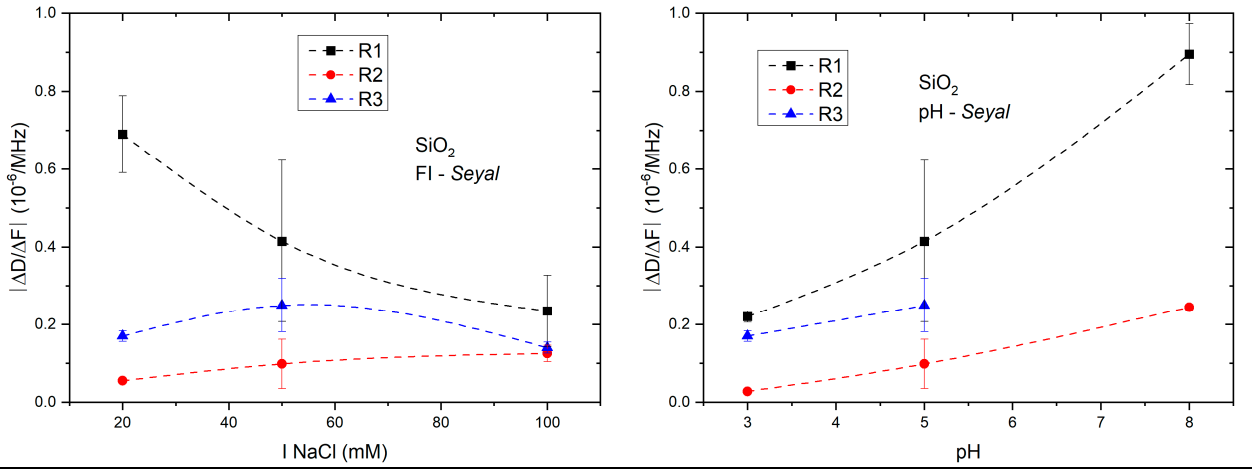

Figure S13. Shear elastic modulus μ (kPa) and shear viscosity η (μPa.s) calculated from QCM-D data for A. *senegal* (up) with the Power law model (PL); and A. *seyal* (down) with both Voigt and Power law models in function of ionic strength in NaCl at pH 5.0 (a) and (b), or in function of pH at 50 mM NaCl (c) and (d) for the three quartz sensors type.

A. senegal – Power law Model

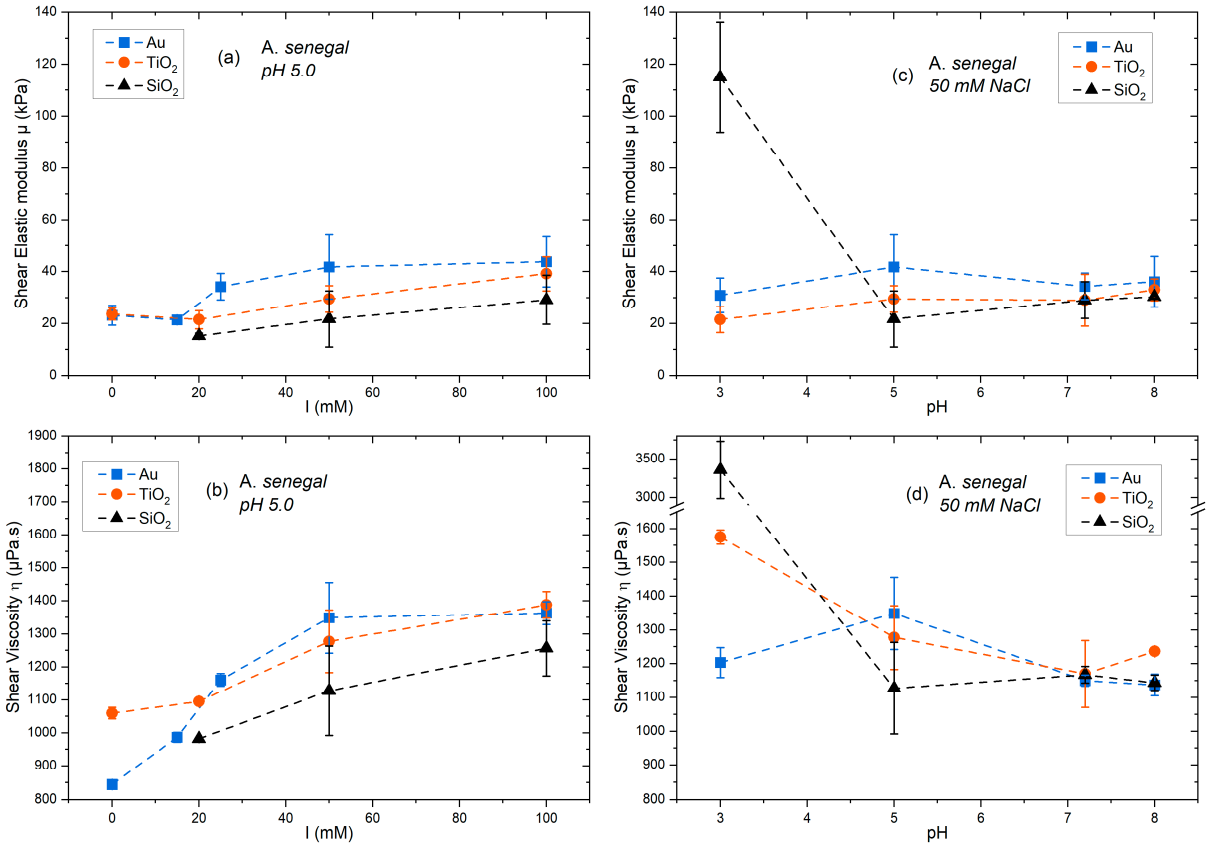

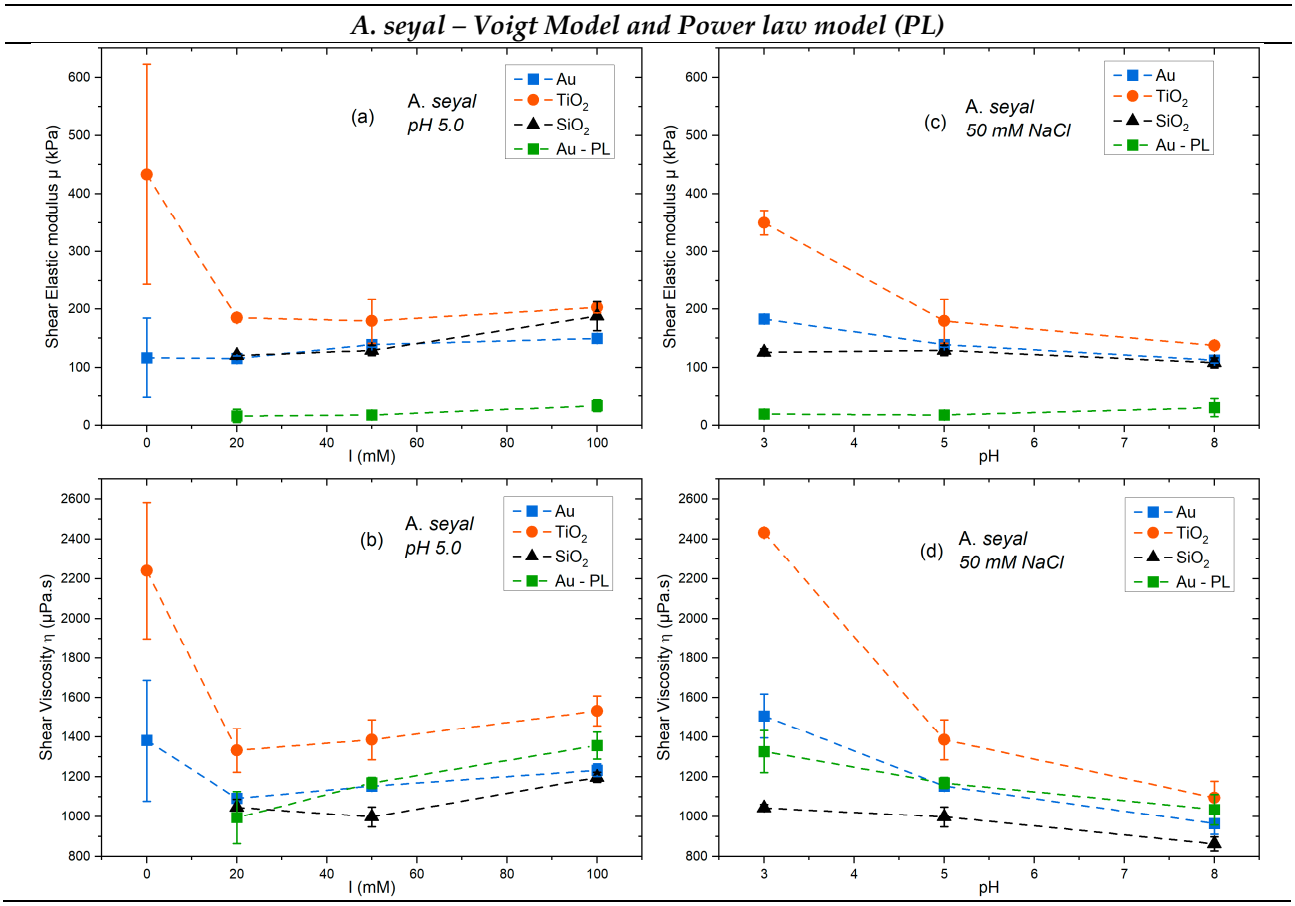

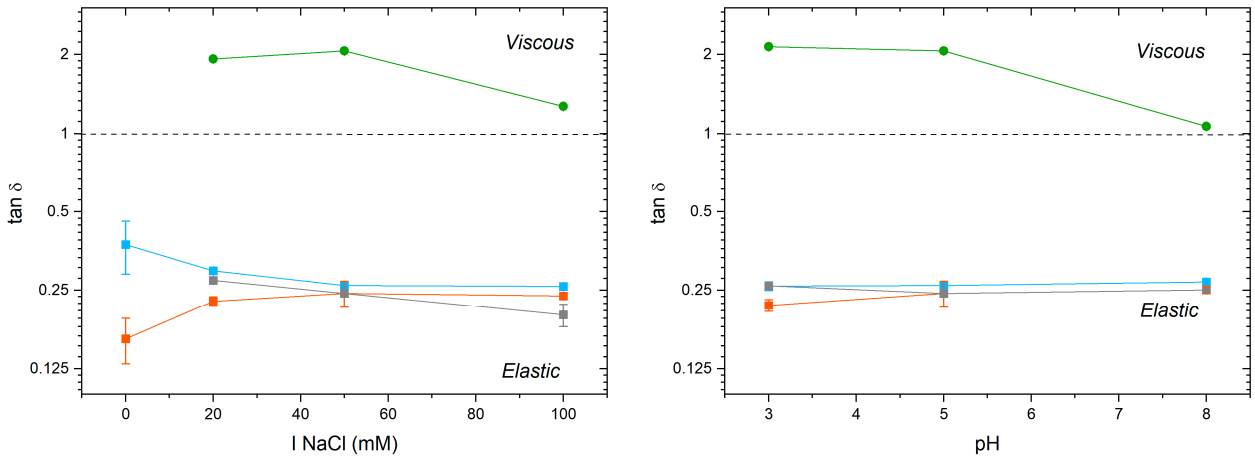

Figure S14. Evolution of tan δ in semi-log scale as a function of ionic strength in NaCl at pH 5.0 (left) or in function of pH at 50 mM NaCl (right) for A. *seyal* (-■-) with the Voigt model onto gold (blue), TiO_2 (orange) or SiO_2 (black) sensors surface compare to (-●-) power law model on gold. *Dashed line is the transition between an elastic and a viscous behavior.*